Tracer diffusion in ordered lattice-gas systems with defect-controlled transport mechanisms

P. Argyrakis,[1] A. A. Chumak,[2] and M. Maragakis[1]
[1]*Department of Physics, University of Thessaloniki, 54124 Thessaloniki, Greece*
[2]*Institute of Physics of the National Academy of Sciences, prospect Nauki 46, Kiev-28, MSP 03028, Ukraine*
(Received 14 April 2007; revised manuscript received 11 July 2007; published 28 August 2007)

Tracer diffusion in an ordered two-dimensional lattice-gas system with square lattice symmetry is studied theoretically and by means of computer simulations. It is well known that the ordering with $c(2\times2)$ symmetry formed in the vicinity of half-filling of lattice sites is due to strong nearest neighbor repulsive interaction. In this case, the tracer migration occurs mainly by elementary displacements of structural defects. This paper focuses on the dimer transport mechanism which was accounted for with insufficient accuracy in previous publications. The long-time asymptotics of the dimer-tracer correlation function (i.e., a three-particle correlation function), which describes concerted tracer-dimer motion, is obtained analytically. We analyze a specific exchange mechanism, relevant to tracer diffusion only. Also, the contribution of generation-recombination jumps to tracer diffusion is taken into account. The theoretical data agree well with the results of intensive Monte Carlo simulations.

DOI: 10.1103/PhysRevB.76.054209 PACS number(s): 64.60.Cn, 68.35.Fx, 68.35.Rh, 05.50.+q

I. INTRODUCTION

The lattice-gas model is widely used to describe adsorption systems.[1–5] This model is quite reasonable when a potential relief of crystal surface represents a set of periodically arranged deep minima for foreign particles. In what follows, the term "particle" means the same as the words "adsorbed particle" and "adatom" which are used in surface science but not in the lattice-gas model. Moreover, the jump mechanism is simplified to a picture where the particle is assumed to spend essentially all of its time localized on lattice sites (potential minima). Accordingly, a relatively insignificant time is needed to complete any jump that it undertakes (during which time the particle is in transit between the relevant two sites). This situation is realized when $e^{-E_A/T}\ll1$, where E_A is the energy required to overcome the barrier between the nearest minima (the activation energy) and T is the temperature in units of k, the Boltzmann constant. There is no unambiguous proof of the full adequacy of the lattice-gas model to any real adsorption system. Nevertheless this model, being quite reasonable from a physical viewpoint, is very simple and useful, for example, for understanding the effects caused by particle-particle interactions.

Usually, there are strong adatom-adatom interactions, which significantly affect the jump probabilities. Therefore, a rigorous theoretical description of the ensemble of strongly interacting particles and derivation of the kinetic coefficients (mobilities and collective diffusion coefficients) are problematic in the general case. Moreover, due to strong particle-particle interaction, these systems undergo phase transitions resulting in the lowering of their symmetry. The theoretical approach[6–8] based on the idea of rapid relaxation to local equilibrium provides an excellent description of the disordered (high-temperature) phase, but it fails to be adequate at undercritical temperatures.[9] The reason for this specific behavior of the low-temperature phase can be easily explained using as an example the ordered systems. The case of antiferromagnetic (checkerboard) ordering is shown in Fig. 1. In a stable ordered state, any particle jump disturbing local ordering induces a force tending to restore the initial order. Hence, the backward jump or other jumps that tend to restore the order are the most probable ones. Therefore, the successive jumps of individual particles in an ordered state are correlated. The approach developed in Ref. 6 completely ignores this circumstance. Realizing the above physical picture, the idea for mass transport description has arisen,[10,11] taking into account the displacements of structural defects.

It has been established that the adsorbate transport occurs as a sequence of displacements of individual structural defects. Each defect displacement is a result of two (or more) strongly correlated elementary jumps of the adsorbed particles. The number of defects is assumed to be small in highly ordered systems. Hence, the problem of mass transport in the ensemble of strongly interacting particles is re-

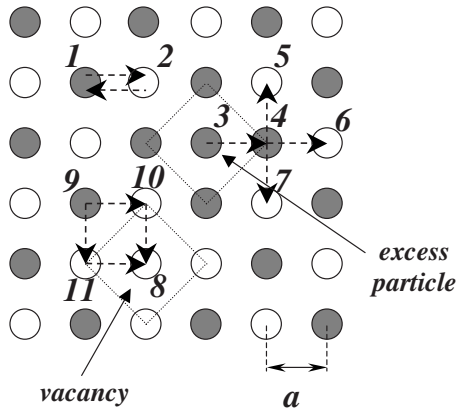

FIG. 1. Schematic of the ordered square lattice. Gray circles: filled sites; open circles: empty sites. Two defect types in site 8 of the filled sublattice and in site 3 of the empty sublattice are shown. The short arrows indicate particle displacements. Two correlated jumps ($1\rightarrow2$ and $2\rightarrow1$) do not contribute to mass transport. Two paths ($9\rightarrow10\rightarrow8$ and $9\rightarrow11\rightarrow8$) show possibilities for vacancy displacement from site 8 to site 9. The displacement of the excess particle from site 3 to one of sites 5, 6, and 7 may occur after the corresponding jump of particle 4 followed by the jump $3\rightarrow4$.

duced to the problem of random walk of almost noninteracting defects. In this way, the correlations of successive jumps are automatically taken into account.

The problem of correlations in ordered systems arises again when one considers tracer diffusion. It is important to emphasize that the analytical description of tracer diffusion is not trivial even in the absence of particle-particle interactions (see, for example, Refs. 12 and 13). In this case, the correlation of successive tracer jumps originates from the exclusion of double occupancy of sites. There is a prevailing probability for the tracer to return to its previous residence site, which remains unoccupied for some time after the tracer jump. This evident correlation of the successive tracer jumps (memory effect) results in the lowering of both the effective jump frequency and the diffusion coefficient of tracers.

A specific case of $c(2\times 2)$ ordering was considered in Ref. 14. The theoretical approach of Ref. 14 is based on both the defect dynamics[10,11] and the procedure of Takhir-Kelly and Elliott[13] modified to be applicable for the case of interacting particles. In Ref. 14, tracer jumps were assumed to occur only due to defect displacements. The case of dominant contribution of single defects to the tracer diffusion was considered quite rigorously. At the same time, an important mechanism of tracer motion, induced by the motion of dimer configurations of defects, was treated only approximately. The approximation of short-range correlations was used. Thus, a rigorous study of tracer-dimer correlations and their influence on tracer diffusion is one of the purposes of the present paper.

Additionally, the importance of generation-recombination (GR) processes of the defects in the adatom kinetics has been established in recent publications.[9,15] In spite of being low-probability events, the GR processes give sizable contribution to the diffusion coefficients at temperatures not much lower than the critical temperature and at filling of the lattice sites close to stoichiometric values. In what follows, we will obtain the tracer diffusion coefficient associated with the GR and exchange jumps. The last type of jumps was not previously analyzed for ordered systems. Each exchange event results in a new particle arrangement with two of their positions being interchanged. Obviously, exchange jumps, resulting from a set of four strongly correlated elementary displacements of adparticles, are relevant to tracer diffusion only, as they do not influence the state of identical particles. The detailed mechanism of the exchange jumps and its importance for tracer motion are explained in Sec. IV.

Concluding this section, it is worth mentioning that a considerable disagreement of theoretical and Monte Carlo (MC) results in the range of understoichiometric coverages was observed in Ref. 14. This circumstance served as a strong motivation for the present study. A reliable theory or exact theoretical results in this field are of great importance since they provide a possibility to test computer algorithms. The combination of intensive MC simulations and a rigorous analytical study which takes into account a variety of effective transport channels for tracer migration will elucidate the reliability of both approaches.

II. DEFECT JUMPS IN THE ORDERED LATTICE

In the vicinity of half-coverage and at sufficiently low temperatures, a lattice-gas system with square symmetry is divided into two sublattices (almost empty and almost filled sublattices). Figure 1 illustrates the particle arrangement in this case. The ideal ordering is disturbed here by the presence of two defects (a vacancy and an excess particle in sites 8 and 3, respectively). The ordering is due to strong nearest neighbor (NN) repulsive interaction. The occupation number of each defect type is given by a simple expression derived in Refs. 10 and 11,

$$n^{v,e} = \mp\left(\theta - \frac{1}{2}\right) + \sqrt{\left(\theta - \frac{1}{2}\right)^2 + e^{-4\varphi}}, \tag{1}$$

where indices v and e denote the corresponding vacancy and excess particle, φ is the dimensionless interaction energy between two nearest neighbors (the interaction energy divided by T), and θ is the average coverage (number of particles per site).

To obtain the probabilities of defect jumps, we need to specify the probability of the elementary jump. It is assumed to be given by the jump frequency

$$\nu_{i,j} = \nu_0 \exp(\epsilon_i), \tag{2}$$

where ν_0 is a constant, i,j are the nearest neighbors, and ϵ_i is the interaction energy of the particle in site i with its nearest neighbors. It is given by $\epsilon_i = \varphi \Sigma_{NN} n_m$, where n_m is the occupancy number, $n_m = (1,0)$, whether the mth site is occupied or not. As we can see, the jump frequency from the ith to jth site, $\nu_{i,j}$, does not depend on the energy of the arrival state j. This site-energy jump probability corresponds to the physical picture where the surrounding particles reduce the potential barrier by ϵ_i. This is a widely used model satisfying detailed balance conditions. It may be improved by taking into account a saddle-point displacement (see, for example, Refs. 5, 16, and 17).

The presence of the exponential factor in Eq. (2) shows the tendency of particles to occupy sites with a minimum value of ϵ. For example, the jump indicated as $1 \rightarrow 2$ in Fig. 1 is followed almost immediately by the reverse $2 \rightarrow 1$ jump. The particle lifetime in site 2 is by a factor $\sim \exp(3\varphi)$ smaller than it is in site 1. These "flip-flop" jumps do not contribute to mass transport, although they may be responsible for short-time correlations of the adsorbate density (see more details in Ref. 18). In contrast to flip-flop jumps, the correlated jumps resulting in the defect displacements are effective in tracer diffusion. Thus, two correlated jumps, $4 \rightarrow 5$ and $3 \rightarrow 4$, result in the excess particle displacement within two elementary vectors. The probability per unit time of each path is equal to $\frac{1}{2}\nu_0 e^{\varphi}$.[10,11] The corresponding probability for vacancies is given by $\frac{1}{2}\nu_0$, i.e., smaller by a factor e^{φ}.

In addition to the motion of isolated defects, such as vacancy 8 and excess particle 4 shown in Fig. 1, dimer configurations of individual defects can also be very effective in mass transfer. Figure 2 illustrates a dimer formed by two excess particles in sites 1 and 2. In this particular configuration, the jumps of particles in sites 3 and 5 are the most probable. It is shown in Fig. 2 that the jump $3 \rightarrow 4$ results in the formation of either 1-4 or 2-4 new dimer configurations. The probability of each event is given by $\frac{1}{3}\nu_0 e^{2\varphi} \equiv \Gamma$.[11] The

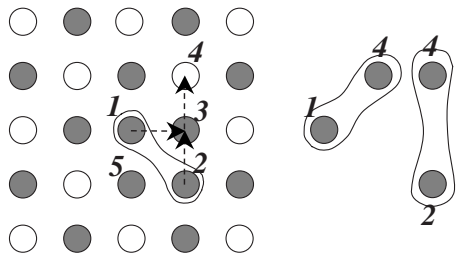

FIG. 2. Schematic of the dimer displacements. After elementary jump $3\rightarrow 4$, particles in sites 1 and 2, as well as particle 4, have equal probabilities to jump to site 3. Two of these jumps result in forming new (1-4) or (2-4) dimer configurations. The new dimers are shown outside the lattice.

dimer concentration n_d is equal to $(n^e)^2$. In spite of the low concentration, the dimers can be effective in migration processes due to very high mobility ($\sim e^{2\varphi}$).

Obviously, the above mechanisms are responsible for migration of tracers (tagged particles). The tracer concentration is assumed to be negligibly small. Hence, it is sufficient to study long-distance displacement of a single tagged particle to obtain the tracer diffusion coefficient.

The consideration of Refs. 10 and 11 uses the assumption of small concentration of the defects. This allows to neglect the interference of different transport mechanisms and to consider separately the contribution of each. Thus, for example, tracer motion due to vacancy jumps is governed by

$$\partial_t \langle n_{\mathbf{i}}^* \rangle = -\frac{1}{2}\nu_0 \sum_{\mathbf{a}\neq -\mathbf{a_1}} \langle n_{\mathbf{i}}^* n_{\mathbf{i+a+a_1}}^v - n_{\mathbf{i+a+a_1}}^* n_{\mathbf{i}}^v \rangle, \tag{3}$$

where $|\mathbf{a}|=|\mathbf{a_1}|=a$, $n_{\mathbf{i}}^*=1,0$ whether or not the $\mathbf{i}$th site is occupied by a tracer, and $n_{\mathbf{i}}^v$ is a similar variable for a vacancy.

As we can see, the evolution of tracer occupancy is governed by a new function $\langle n_{\mathbf{i}}^* n_{\mathbf{i+a+a_1}}^v \rangle$, which describes tracer-vacancy correlations. The evolution of the correlation function is governed by a linear equation, which can be easily derived similarly to Eq. (3). Its linearity is due to the small vacancy concentration. The authors of Ref. 14 have managed to solve this equation. In the limit of asymptotically long time, when the tracer evolution can be described by the diffusion equation, the tracer-dimer correlation function was expressed in terms of $n_{\mathbf{i}}^*$. Then, its substitution into Eq. (3) gives the possibility to obtain the tracer diffusion coefficient in the case of vacancy transport mechanism, D_v^*. It is given by

$$D_v^* = 4D_0 n^v 0.63, \tag{4}$$

where $D_0=\nu_0 a^2$.

A similar analysis is applicable in the case of tracer diffusion due to excess particles. The corresponding value of the diffusion coefficient was obtained in Ref. 14 to be equal to

$$D_e^* = 4D_0 n^e e^{\varphi} 0.725. \tag{5}$$

The effect of the dimers on tracer diffusion was also considered in Ref. 14. The analytical solution is rather complicated because it describes the correlated motion of three particles. To simplify the task, the approximation of short-range correlations was used. This approach implies that the tracer-dimer correlations are negligibly small if any tracer-defect spacing is greater than a (we mean only defects which are constituents of the dimer). In the next section, we will consider rigorously concerted tracer-dimer motion (in the spirit of the tracer–single-defect theory). Thus, it will become possible to compare the results of both approaches.

III. RATE EQUATIONS FOR CORRELATED TRACER-DIMER MOTION

We consider here tracer displacements caused by dimer motion. It can be easily seen from Fig. 2 that a tracer jump may occur if it is initially in one of positions 1, 2, 3, and 5. In other words, the tracer jump is possible only if it is a constituent of the dimer or if it is a NN of both defects (1 and 2).

We proceed from the equation of occupancy evolution of the ith site in the filled sublattice and its NN sites in the empty sublattice, namely,

$$n_{\mathbf{i}}^* + \frac{1}{4}\sum_{\mathbf{a}} n_{\mathbf{i+a}}^*. \tag{6}$$

It is convenient to introduce the notation for the dimer variables: $n_{\mathbf{i}}^{\mathbf{j}}$ denotes the dimer formed by the pair of defects in sites $\mathbf{i}$ and $\mathbf{j}$ of the empty sublattice (the defects are away from one another by a distance not longer than $2a$: $|\mathbf{i}-\mathbf{j}|=\sqrt{2}a$ or $2a$); $n_{\mathbf{i}*}^{\mathbf{j}}$ means that the tracer is the constituent of the dimer (the defect in site i is formed by a tagged particle).

Then, the rate equation corresponding to the above described mechanism of the tracer displacements is given by

$$\partial_t \left\langle \left(n_{\mathbf{i}}^* + \frac{1}{4}\sum_{\mathbf{a}} n_{\mathbf{i+a}}^* \right) \right\rangle = \frac{3}{2}\Gamma \sum \langle n_{\mathbf{i+a}^*}^{\mathbf{i+a_1}} - n_{\mathbf{i}}^* n_{\mathbf{i+a}}^{\mathbf{i+a_1}} \rangle + \frac{\Gamma}{4}\sum \langle n_{\mathbf{i+a+a_1}}^* n_{\mathbf{i+a+a_1+a_3}}^{\mathbf{i+a+a_1+a_3}} - n_{\mathbf{i+a}^*}^{\mathbf{i+a+a_1+a_2}} \rangle. \tag{7}$$

The first sum in the right part runs over vectors $\mathbf{a},\mathbf{a_1}$ excluding the terms with $\mathbf{a}=\mathbf{a_1}$. The second sum runs over vectors $\mathbf{a},\mathbf{a_1},\mathbf{a_2},\mathbf{a_3}$ excluding the terms with $\mathbf{a},\mathbf{a_2},\mathbf{a_3}=-\mathbf{a_1}$ and $\mathbf{a_2}=\mathbf{a_3}$.

As we can see, the evolution of the tracer occupancy depends on the joint probabilities of the tracer and a dimer to be in close vicinity. For further analysis, it is convenient to introduce new functions g and d defined as

$$g(\mathbf{i},\mathbf{r},\mathbf{A}) = \langle n_{\mathbf{i}}^* (n_{\mathbf{i+r}}^{\mathbf{i+r+A}} - n_d) \rangle, \tag{8}$$

where vectors $\mathbf{i}$ and $\mathbf{r}$ belong to the "filled" and "empty" sublattices, respectively, and

$$d(\mathbf{i},\mathbf{A}) = \langle n_{\mathbf{i}*}^{\mathbf{i+A}} - n_{\mathbf{i}}^* n_d \rangle. \tag{9}$$

Here, vector $\mathbf{i}$ denotes a site in the empty sublattice. Vector $\mathbf{A}$ indicates the dimer configuration, $\mathbf{A}=\mathbf{a}+\mathbf{a}'$, $|\mathbf{A}|\leqslant 2a$.

The quantity $g(\mathbf{i},\mathbf{r},\mathbf{A})$ is the tracer-dimer correlation function, where the variable $\mathbf{r}$ determines the spatial separation of these objects. The other function, $d(\mathbf{i},\mathbf{A})$, describes a dimer configuration, where one of the excess particles (in site $\mathbf{i}$) is a tracer.

In further analysis, we will use an important property of function g, namely,

$$g(\mathbf{i},\mathbf{r},\mathbf{A}) = g(\mathbf{i},\mathbf{r}+\mathbf{A},-\mathbf{A}), \tag{10}$$

which follows directly from definition (8). For the Fourier transform defined by

$$g_{\mathbf{k}}(\lambda,\mathbf{A}) = \sum_{\mathbf{i},\mathbf{r}} e^{i(\lambda\mathbf{r}-i\mathbf{k})} g(\mathbf{i},\mathbf{r},\mathbf{A}), \tag{11}$$

this property is expressed by

$$g_{\mathbf{k}}(\lambda,\mathbf{A}) = g_{\mathbf{k}}(\lambda,-\mathbf{A}) e^{-i\lambda\mathbf{A}}. \tag{12}$$

It is assumed here that $g(\mathbf{i},\mathbf{r},\mathbf{A})$ and $d(\mathbf{i},\mathbf{A}) \to 0$ when $|\mathbf{i}| \to \infty$, and $g(\mathbf{i},\mathbf{r},\mathbf{A}) \to 0$ when $|\mathbf{r}| \to \infty$. The last property implies the decay of tracer-dimer correlations with increasing of the separation between them.

Also, it is evident that

$$g_{\mathbf{k}=0}(\mathbf{r},\mathbf{A}) = d_{\mathbf{k}=0}(\mathbf{r}) = 0, \tag{13}$$

where $d_{\mathbf{k}}(\mathbf{A}) = \Sigma_{\mathbf{i}} e^{-i\mathbf{k}\mathbf{i}} d(\mathbf{i},\mathbf{A})$. Equation (13) follows from the observation that the probability to obtain the dimer at a given state does not depend on the tracer position.

Now, Eq. (7) can be rewritten as

$$(1/\Gamma)\partial_t \left\langle n_{\mathbf{i}}^* + \frac{1}{4}\sum_{\mathbf{a}} n_{\mathbf{i}+\mathbf{a}}^* \right\rangle_{\mathbf{k}} = -12(ka)^2 n_d \langle n_{\mathbf{k}}^* \rangle - i\mathbf{k} \sum_{\mathbf{a}\neq\mathbf{a}_1} \left[(\mathbf{a}+\mathbf{a}_1) g_{\mathbf{k}}(\mathbf{a},\mathbf{a}_1-\mathbf{a}) - \frac{3}{2}(\mathbf{a}-\mathbf{a}_1/3) d_{\mathbf{k}}(\mathbf{a}_1-\mathbf{a}) \right]. \tag{14}$$

As we can see from Eq. (14), in order to obtain the diffusion coefficient of tracers, it is sufficient to know the functions $g_{\mathbf{k}}(\mathbf{r}=\mathbf{a},\mathbf{A})$ and $d_{\mathbf{k}}(\mathbf{A})$ in the lowest order in $\mathbf{k}$. In view of Eq. (13), these functions may be linear or of higher order in $\mathbf{k}$. The evolution equations determining functions g and d can be derived in a manner similar to that for Eq. (14). Then, taking into account only the linear terms in $\mathbf{k}$, we get

$$\frac{1}{\Gamma}\partial_t g_{\mathbf{k}}(\lambda,\mathbf{a}+\mathbf{a}_1) = \left(1-\frac{1}{2}\delta_{\mathbf{a},\mathbf{a}_1}\right)\Big\{-8g_{\mathbf{k}}(\lambda,\mathbf{a}+\mathbf{a}_1) + \sum_{\mathbf{a}_2\neq-\mathbf{a},\mathbf{a}_1} [g_{\mathbf{k}}(\lambda,\mathbf{a}+\mathbf{a}_2)(1+e^{-i\lambda(\mathbf{a}_1-\mathbf{a}_2)}) + g_{\mathbf{k}}(\lambda,\mathbf{a}_1-\mathbf{a}_2)(1+e^{-i\lambda(\mathbf{a}+\mathbf{a}_2)}) + e^{-i\lambda\mathbf{a}}(d_{\mathbf{k}}(\mathbf{a}_1-\mathbf{a}_2) + d_{\mathbf{k}}(-\mathbf{a}-\mathbf{a}_2) - g_{\mathbf{k}}(-\mathbf{a},\mathbf{a}+\mathbf{a}_2) - g_{\mathbf{k}}(\mathbf{a}_2,\mathbf{a}_1-\mathbf{a}_2)) + e^{-i\lambda\mathbf{a}_1}(d_{\mathbf{k}}(\mathbf{a}+\mathbf{a}_2) + d_{\mathbf{k}}(\mathbf{a}_2-\mathbf{a}_1) - g_{\mathbf{k}}(\mathbf{a},-\mathbf{a}-\mathbf{a}_2) - g_{\mathbf{k}}(-\mathbf{a}_2,\mathbf{a}_2-\mathbf{a}_1))] + 2i\mathbf{k}(\mathbf{a}-\mathbf{a}_1) n_{\mathbf{k}}^* n_d (e^{-i\lambda\mathbf{a}} - e^{-i\lambda\mathbf{a}_1})\Big\} \tag{15}$$

and

$$\frac{1}{\Gamma}\partial_t d_{\mathbf{k}}(\mathbf{a}+\mathbf{a}_1) = \left(1-\frac{1}{2}\delta_{\mathbf{a},\mathbf{a}_1}\right)\Big\{-8d_{\mathbf{k}}(\mathbf{a}+\mathbf{a}_1) + \sum_{\mathbf{a}_2\neq-\mathbf{a},\mathbf{a}_1} [d_{\mathbf{k}}(\mathbf{a}+\mathbf{a}_2) + d_{\mathbf{k}}(\mathbf{a}_1-\mathbf{a}_2) + g_{\mathbf{k}}(\mathbf{a},-\mathbf{a}-\mathbf{a}_2) + g_{\mathbf{k}}(\mathbf{a}_2,\mathbf{a}_1-\mathbf{a}_2)] + 2i\mathbf{k}(\mathbf{a}+\mathbf{a}_1) n_{\mathbf{k}}^* n_d\Big\}, \tag{16}$$

where properties (10) and (12) were used.

A set of 16 Eqs. (15) and (16) can be solved straightforwardly. At the first step, $g_{\mathbf{k}}(\lambda,\mathbf{A})$ is expressed in terms of $n_{\mathbf{k}}^*$ and $g_{\mathbf{k}}(\mathbf{a},\mathbf{a}_{\mathbf{j}}-\mathbf{a})$. Then, by means of reverse Fourier transforming from λ to $\mathbf{r}$ domain, the functions $g_{\mathbf{k}}(\mathbf{a},\mathbf{a}_{\mathbf{j}}-\mathbf{a})$, which enter the right-hand part of Eq. (14), will be obtained. The procedure can be simplified by considering the symmetry properties of the system. First of all, the linear in $\mathbf{k}$ term of $d_{\mathbf{k}}(\mathbf{a}+\mathbf{a}_{\mathbf{j}})$ can be represented by

$$d_{\mathbf{k}}(\mathbf{a}+\mathbf{a}_{\mathbf{j}}) = D\mathbf{k}(\mathbf{a}+\mathbf{a}_{\mathbf{j}}), \tag{17}$$

where D does not depend on $\mathbf{k}$. In a similar manner, we may set $g_{\mathbf{k}}(\mathbf{a},\mathbf{a}_{\mathbf{j}}-\mathbf{a}) = G_1\mathbf{k}\mathbf{a} + G_2\mathbf{k}(\mathbf{a}_{\mathbf{j}}-\mathbf{a})$. The constants G_1 and G_2 are not independent. It follows from Eq. (10) that $G_1 = 2G_2 \equiv 2G$. Thus, we have

$$g_{\mathbf{k}}(\mathbf{a},\mathbf{a}_{\mathbf{j}}-\mathbf{a}) = G\mathbf{k}(\mathbf{a}+\mathbf{a}_{\mathbf{j}}). \tag{18}$$

Using Eqs. (15)–(18), we can easily obtain

$$g_{\mathbf{k}}(\lambda,\mathbf{a}+\mathbf{a}_1) = S/R, \tag{19}$$

where $\mathbf{a} \perp \mathbf{a}_1$,

$$S = 2(in_{\mathbf{k}}^* n_d - 2D)\mathbf{k}\{(\mathbf{a}+\mathbf{a}_1)3(\cos\lambda\mathbf{a} + \cos\lambda\mathbf{a}_1) \times [e^{-i\lambda(\mathbf{a}+\mathbf{a}_1)} - 1] + (\mathbf{a}-\mathbf{a}_1)[e^{-i\lambda\mathbf{a}} - e^{-i\lambda\mathbf{a}_1}] \times [7 - \cos\lambda(\mathbf{a}+\mathbf{a}_1)]\},$$

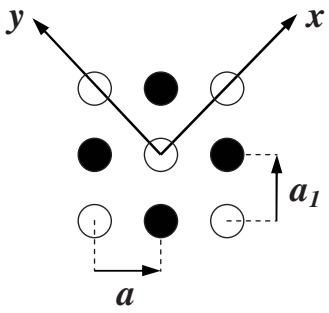

FIG. 3. Axes orientation.

$$R = [7 - \cos\lambda(\mathbf{a} - \mathbf{a_1})][7 - \cos\lambda(\mathbf{a} + \mathbf{a_1})] - 9(\cos\lambda\mathbf{a} + \cos\lambda\mathbf{a_1})^2, \quad (20)$$

and

$$D = \frac{1}{3}(G + in_d n_{\mathbf{k}}^*). \quad (21)$$

The function $g_{\mathbf{k}}(\lambda, 2\mathbf{a})$ is expressed in terms of $g_{\mathbf{k}}(\lambda, \mathbf{a} \pm \mathbf{a_1})$ as

$$g_{\mathbf{k}}(\lambda, 2\mathbf{a}) = \frac{1}{4}[g_{\mathbf{k}}(\lambda, \mathbf{a} + \mathbf{a_1})(1 + e^{i\lambda(\mathbf{a_1} - \mathbf{a})}) + g_{\mathbf{k}}(\lambda, \mathbf{a} - \mathbf{a_1})(1 + e^{-i\lambda(\mathbf{a} + \mathbf{a_1})})]. \quad (22)$$

When deriving Eqs. (19)–(22), we have neglected the left-hand parts of Eqs. (15) and (16). The reason for this is as follows. We are seeking for long-time asymptotic values of correlation functions, which describe diffusionlike migration (slow migration) of the tracer. The characteristic time of the tracer density evolution can be estimated from Eq. (14) to be equal to $\Gamma(ka)^2$. Hence, the characteristic value of the term $\frac{1}{\Gamma}\partial_t g$ can be considered to be given by $(ka)^2 g$, which is much less than the corresponding terms in the right part of Eq. (15). A similar reasoning is also applicable to Eq. (16).

Now, we are able to obtain the contribution of the dimer motion to the tracer diffusion coefficient D_d^*. Using Eqs. (19)–(22) and Fourier transforming from λ to $\mathbf{r}$ domain, Eq. (14) can be rewritten in the form

$$\partial\langle n_{\mathbf{k}}^*\rangle = -D_d^* k^2 \langle n_{\mathbf{k}}^*\rangle, \quad (23)$$

where

$$D_d^* = D_0 n_d e^{2\varphi} \frac{20/9}{1 - \Psi},$$

$$\Psi = \frac{8}{3N}\sum_{\lambda} \frac{1}{R}[7 - \cos\lambda(\mathbf{a} + \mathbf{a})][1 - \cos\lambda(\mathbf{a} - \mathbf{a_1})].$$

It is taken into account here that the probability of a tracer to occupy a site in the filled sublattice is much greater than that in the empty sublattice.

For numerical summation, it is convenient to choose the coordinate system rotated at $\pi/4$ with respect to the basic lattice vectors as indicated in Fig. 3. In this case, $\lambda(\mathbf{a} \pm \mathbf{a_1}) = \pm\lambda_{x,y} a\sqrt{2}$, where $\lambda_{x,y}$ takes the values $2\pi n_{x,y}/(a\sqrt{N})$ ($n_{x,y} = 1, 2, \ldots, \sqrt{N/2}$ and N is the total number of the lattice sites). For a sufficiently large system, when Ψ does not depend on N, we get $\Psi \approx 0.2186$, and

$$D_d^* = 4D_0 n_d e^{2\varphi} 0.711. \quad (24)$$

As we can see, the numerical number 0.711 is a result of summation of the explicit expression for ψ. The coefficients 0.63 and 0.725 in Eqs. (4) and (5) are of similar origin (see Ref. 14).

The previous theories provide different numerical coefficients in the expression for D_d^*, namely, (i) the approach of Refs. 10 and 11, which neglects the tracer-dimer correlations, results in numerical coefficient 1 instead of 0.711 and (ii) the theory of Ref. 14, where only short-range correlations are accounted for, gives 0.53 instead of 0.711. As we can see, the difference is quite sizable in both cases.

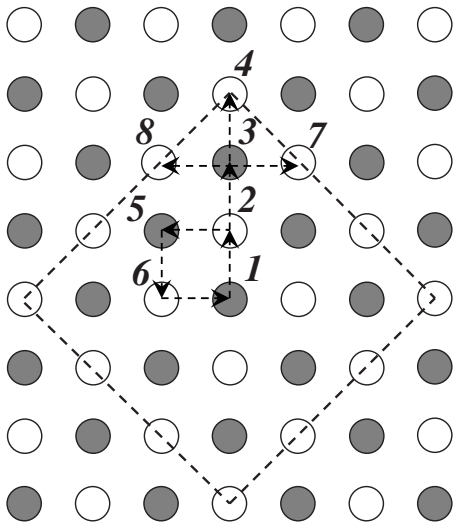

FIG. 4. A set of three sequential jumps, $1 \rightarrow 2$, $3 \rightarrow 4$, and $2 \rightarrow 3$, results in the creation of two defects (a vacancy in site 1 and an excess particle in site 4). The dashed lines indicate 12 possible positions of the excess particle if a vacancy appears in site 1. A set of four jumps, $1 \rightarrow 2$, $5 \rightarrow 6$, $6 \rightarrow 1$, and $2 \rightarrow 5$, illustrates the exchange mechanism: the initial particle positions 1 and 5 become interchanged.

IV. CONTRIBUTION OF EXCHANGE JUMPS AND GENERATION-RECOMBINATION JUMPS

A perfect ordering is impossible if coverage θ is not equal to 0.5. For $\theta > 0.5$, some particles occupy the empty lattice, forming defects which are named here as excess particles. When $\theta < 0.5$, vacancies appear in the filled lattice. At the same time, some amount of defects is thermally generated in both sublattices. There always exist specific sequences of the adparticle jumps resulting in generation (recombination) events. Balance conditions for generation and recombination rates establish equilibrium numbers of the defects [see Eq. (1)]. Being events of low probability, the GR jumps may be also effective in the mass transfer at not too low temperatures (see the results of Refs. 9 and 15 for three-dimensional and

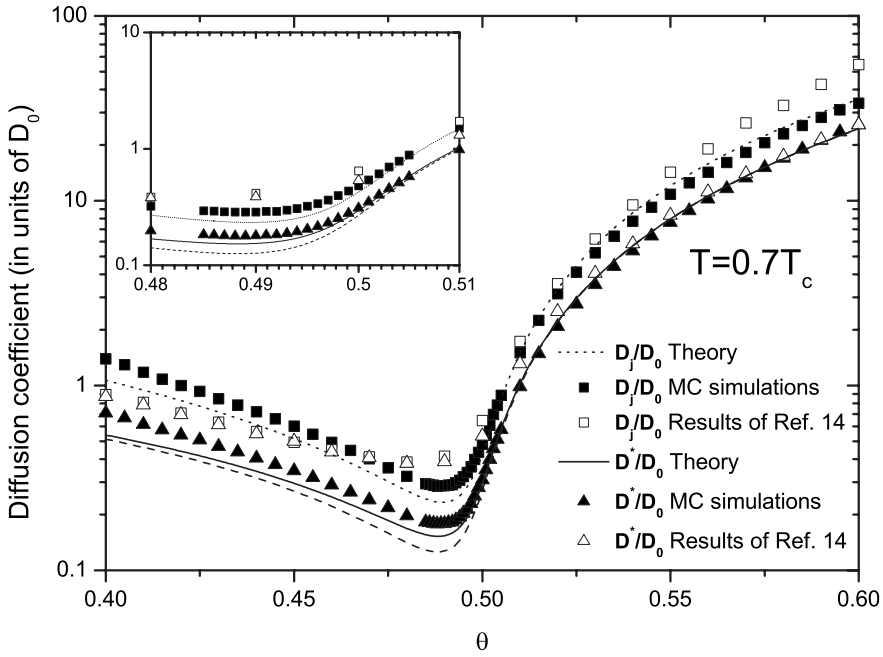

FIG. 5. Theoretical and Monte Carlo data for the tracer and jump diffusion coefficients vs coverage θ. The temperature $T=0.7T_c$ corresponds to $\varphi \approx 2.514$. The dashed line shows the theoretical values without the contribution of exchange and GR jumps. The inset shows the detail of the area near the minima of the diffusion coefficient.

two-dimensional lattice systems, respectively).

Figure 4 illustrates a sequence of jumps resulting in a defect pair creation. After starting elementary jump $1 \rightarrow 2$, the most probable is the reverse jump because the particle in site 3 has three NN adparticles. Nevertheless, a low probability $3 \rightarrow 4$ jump followed by $2 \rightarrow 3$ jump is also possible. The effective jump frequency corresponding to the above set of jumps (resulting in the creation of the vacancy in site 1 and the excess particle in site 4) is given by $\nu_0 e^{-3\varphi}$.[11] The paths $1 \rightarrow 2$, $3 \rightarrow 7$, $2 \rightarrow 3$ and $1 \rightarrow 2$, $3 \rightarrow 8$, $2 \rightarrow 3$ have the same probabilities. The dashed lines indicate sites where excess particles may appear after the vacancy generation in site 1.

There is another scenario of particle displacements after the $1 \rightarrow 2$ jump. It starts from the $5 \rightarrow 6$ jump. Further rearrangement follows by one of four equal-probability paths. These are (i) jumps $6 \rightarrow 1$ and $2 \rightarrow 5$, (ii) jumps $2 \rightarrow 5$ and $6 \rightarrow 1$, jumps $6 \rightarrow 5$ and $2 \rightarrow 1$, and jumps $2 \rightarrow 1$ and $6 \rightarrow 5$. It can be easily seen that the former two sets result in a new state of the system with particle positions in sites 1 and 5 interchanged. The last two sets return the system to the initial state. The effective jump frequency corresponding to the interchange event, which begins with the $1 \rightarrow 2$ jump, is equal to $\frac{1}{2}\nu_0 e^{-2\varphi}$. The same interchange may occur in the case of starting with $1 \rightarrow 6$ jump (a set of clockwise particle jumps). Then, the overall frequency of interchange events between two given sites, ν_{ech}, is twice as much, i.e., $\nu_0 e^{-2\varphi}$.

Having obtained the rate of the exchange jumps, we can easily calculate their contribution to the tracer diffusion coefficient D^*_{exch}. It is given by

$$D^*_{exch} = 2D_0 e^{-2\varphi}. \tag{25}$$

This value corresponds to the collective diffusion coefficient of free particles moving on a lattice with the period $\sqrt{2}a$ and having the jump frequency $\nu_0 e^{-2\varphi}$.

The tracer migration caused by GR jumps can be described by an approximate procedure developed in Refs. 9 and 15. According to this approach, the generation of two defects in sites 1 and 4 is accompanied with the tracer displacements $1 \rightarrow 3$ or $3 \rightarrow 4$ (if initially they are available there). A similar approach can be applied to the recombination jumps. A very simple analysis results in the tracer diffusion coefficient caused by GR processes, D^*_{GR}, being equal to

$$D^*_{GR} = 27 D_0 e^{-3\varphi}. \tag{26}$$

Finally, with regard to Eqs. (4), (5), and (24)–(26), we have the following for the tracer diffusion coefficient:

$$\begin{aligned} D^* &= D^*_v + D^*_e + D^*_d + D^*_{exch} + D^*_{GR} \\ &= 4D_0 \Big[0.63 n^v + 0.725 n^e e^{\varphi} + 0.711 (n^e e^{\varphi})^2 \\ &\quad + 0.5 e^{-2\varphi} + \frac{27}{4} e^{-3\varphi} \Big]. \end{aligned} \tag{27}$$

The terms in brackets are due to different transport mechanisms. They are connected with the motion of vacancies, excess particles, and dimers, as well as with the exchange and GR jumps. It follows that the contribution of GR and exchange jumps becomes negligible when $\varphi \rightarrow \infty$.

V. DISCUSSION

In Figs. 5 and 6 we plot the diffusion coefficients vs the coverage θ for two different values of T/T_c. The ratio T/T_c is equal to φ_c/φ, where the critical value of the interaction parameter φ_c is equal to 1.76 for a square lattice. We observe

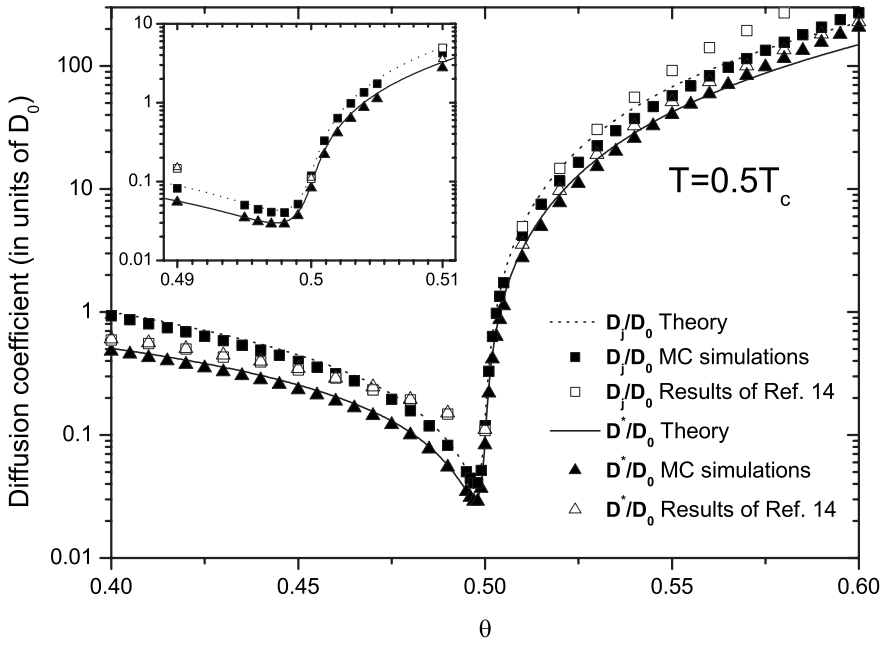

FIG. 6. The same as in Fig. 5 but for $T=0.5T_c$ ($\varphi \approx 3.52$).

some very pronounced minima at coverage close to the stoichiometric value, $\theta=0.5$, which are due to the small number of the defects. For this reason, the exchange and GR jumps become competitive here (see, for comparison, the dashed line in Fig. 5). Their relative contributions can be easily calculated with the use of Eqs. (1) and (27). In the vicinity of the minimum, they amount to 8% at $T=0.5T_c$ and 18% at $T=0.7T_c$ of the total value of D^*.

One can guess that some other complex jumps will occur when $T \to T_c$. However, the near-critical dynamics of the lattice-gas system is not a subject of the present paper. Our approach may be considered as heuristic and it is based on the assumption $e^{-\varphi} \ll 1$. It does not indicate a direct way of the development of the theory in close vicinity to the critical point, where another small quantity $|T-T_c|/T$ should be the most important physical quantity determining critical dynamics of the system.

The minima in the diffusion coefficients were obtained at first in Ref. 19 by means of MC simulations. Later on, they were interpreted in Refs. 10 and 11 as a crossover point from vacancy to excess particle transport mechanism.

The Monte Carlo simulations included here are in the same spirit as in our previous publications.[15,18] The lattice size used was 100×100. The following considerations were taken into account just for this choice. On one hand, this size must be sufficiently large to avoid the finite-size effect. On the other hand, it should not be too large because of the restricted computer resources. It is evident that finite-size effects can lead to complications in the vicinity of half-coverage where the number of defects is minimum. It can affect the recombination rate of the defects. Our simulations use periodic boundary conditions, so when each particle crosses the boundary, it automatically appears at the opposite boundary. Therefore, two defects can recombine in two ways: (i) moving one toward another and (ii) starting a motion in almost opposite directions with a subsequent crossing of the boundary. As a result, the overall recombination rate increases. Taking into account that the generation rate is not affected by the boundaries, we can conclude that the stationary concentration of defects is lower for small lattice sizes. The effect of boundaries on the stationary concentration of the defects is negligible when the number of defects is large, i.e., when $(N/2)e^{-2\varphi} \gg 1$. This number is equal to 33 for $T=0.7T_c$ and 4.4 for $T=0.5T_c$. It is important to emphasize that these estimates concern only a small vicinity of the stoichiometric coverage, 0.5, where $|\theta-0.5|$ is of the order of or less than 0.01 in the first case and 0.002 in the second. Out of this range, the finite-size effects are much smaller. Due to the slow evolution of the system and the small number of jumps per MC step, typically 10^7 MC steps were performed per individual initial configuration. The results were also averaged over 50 independent realizations.

The behavior of diffusion coefficients to the left of the minima is controlled mainly by the vacancy mechanism, while to the right, the behavior is controlled by excess particles and their dimers. In general, the dependence of the tracer diffusion coefficient on θ is similar to that of the jump diffusion coefficient D_J. The explicit term for D_J (with account for GR jumps) can be deduced from Refs. 11 and 15. It is given by

$$D_J = \frac{2}{\theta} D_0 \left[n^v + n^e e^{\varphi} + \frac{4}{3}(n^e e^{\varphi})^2 + \frac{39}{2} e^{-3\varphi} \right]. \qquad (28)$$

There are at least two evident reasons why D^* and D_J should be different: (i) tracer diffusion is a result of correlated tracer-defect motion, while the jump diffusion coefficient (the particle mobility) is determined by free motion of defects only; (ii) for most types of defect displacements, the tracer jump is shorter than the corresponding length of mass

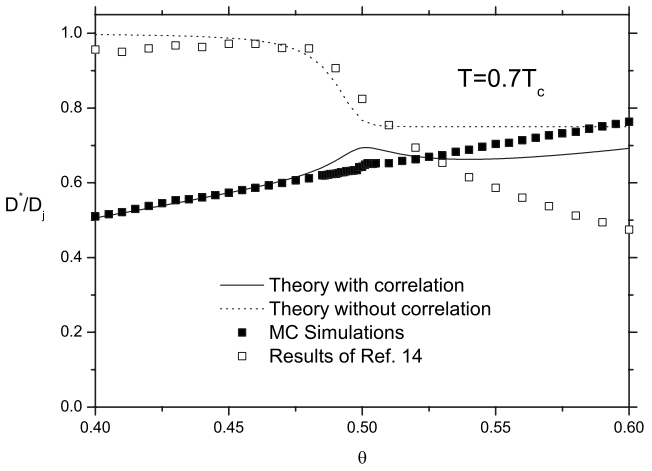

FIG. 7. Ratio of tracer to jump diffusion coefficients for $T=0.7T_c$.

displacement. Figures 5 and 6 illustrate good agreement of the theoretical and MC data for both quantities, D_J and D^*.

It follows from the above that the ratio of tracer to jump diffusion coefficients provides information about tracer-defect correlations. In Figs. 7 and 8, we see good agreement between theoretical and MC data in the range of $\theta \leqslant 0.5$. At the same time MC data of Ref. 14 disagree with both significantly. The MC results of Ref. 14 correspond to early theoretical data of Refs. 10 and 11 obtained with the approach where tracer-defect correlation is neglected. The agreement of the simplified theoretical version with the results of MC simulations may happen if the number of MC steps per run is not sufficiently large to ensure many tracer jumps in each run. In this case, the averaging over many runs is equivalent to the theoretical model[10,11] in which any tracer jump is due to the average number of defects. Such simulation procedure does not provide information about tracer-vacancy correlations and, in fact, neglects it like the simplified early theories.

A good agreement of the theory and simulations in the region of $\theta \approx 0.5$ has a very simple explanation. Our theory provides the best results just in the vicinity of $\theta=0.5$, where the number of the defects is minimum. The "contacts" of defects are negligible here. On the other hand, we have succeeded with sufficient statistics even in this region of almost "frozen" order, since, specifically in this region, we have allowed for 2×10^7 MC steps in our simulations.

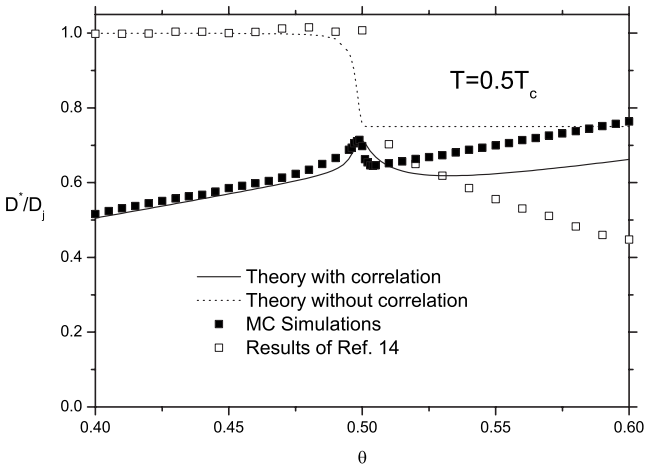

FIG. 8. The same as in Fig. 8 but for $T=0.5T_c$.

In the region of $\theta > 0.5$, where the excess particle and dimer transport mechanisms dominate, the agreement is not so good. Further outside from the center, we see a sizable difference between the theoretical and numerical data. This takes place in the region where the dimer motion is no longer a free motion. The individual dimer responsible for the previous tracer displacements can meet an excess particle or another dimer and disintegrate. The many-particle problem appears here again. If the dimer lifetime is of the order of or less than the tracer-dimer correlation time, the correlation effect decreases. The theoretical version with tracer-defect correlations neglected becomes preferable here. The MC results support this point. We see the agreement of MC data with results of the old theory at $\theta=0.6$ (the number of excess particles per site in the empty sublattice is ≈ 0.2). Concluding this section, a finite lifetime of the dimers should be taken into account to get a good theoretical description at $\theta > 0.5$.

VI. CONCLUSION

Our motive in this study was to elucidate the physical mechanisms responsible for tracer diffusion in a specifically ordered system by bringing together theoretical and MC approaches. Various correlation phenomena are connected with the tracer long-distance displacements. The tracer diffusion coefficient is mainly controlled by jumps of three types of structural defects. These are the vacancies, excess particles, and dimer configurations of the excess particles. The defect jumps occur as two strongly correlated elementary jumps of the adsorbed particles. In contrast to the jump diffusion coefficient, it is the tracer-defect correlated motion that determines the tracer diffusion and not only the free motion of the defects. This specific correlation makes the theoretical analysis more difficult. Nevertheless, it is still possible. In addition to previous theoretical studies, we have derived here analytically the explicit form of the three-particle correlation function, which describes the concerted motion of tracers and dimers.

Additionally, we have accounted for the GR and exchange jumps, which sometimes are also important for tracer migration. In antiferromagnetically ordered systems, the exchange jumps are considered at first. The GR and exchange jumps occur as a result of three and four correlated successive jumps of adparticles, respectively.

The present results of the large-scale simulations support the importance of the tracer-defect correlation (or long-time memory effect) predicted theoretically. To establish this important point, we have studied the coverage dependence of the D^*/D_J ratio. This quantity is very sensitive to correlation effects and its reliable calculation requires considerable computational efforts. Nevertheless, good agreement between

MC and theoretical data in the range $\theta \leqslant 0.5$ is reached. This is in contrast to results of Ref. 14, where the essential difference between the two was observed, and the MC data rather supported the absence of tracer-defect correlation. Also, our data show the ratio D^*/D_J as a growing function of θ when $\theta > 0.5$, while in Ref. 14, it was a monotonically decreasing function.

ACKNOWLEDGMENTS

This work was partially supported by project PENED 03ED840 (Greek General Secretariat for Research and Technology), Interreg IIIA CBC No. 102646 and Ukrainian project VTS/138 (Nanophysics).

[1] J. W. Haus and K. W. Kehr, Phys. Rep. **150**, 263 (1987).
[2] *Surface Diffusion: Atomistic and Collective Processes*, edited by M. C. Tringides (Plenum, New York, 1998).
[3] J. V. Barth, Surf. Sci. Rep. **40**, 75 (2000).
[4] T. Ala-Nissila, R. Ferrando, and S. C. Ying, Adv. Phys. **51**, 949 (2002).
[5] M. A. Zaluska-Kotur and Z. W. Gortel, Phys. Rev. B **72**, 235425 (2005).
[6] A. A. Chumak and A. A. Tarasenko, Surf. Sci. **91**, 694 (1980).
[7] D. A. Reed and G. Ehrlich, Surf. Sci. **105**, 603 (1981).
[8] V. P. Zhdanov, Surf. Sci. Lett. **149**, L13 (1985).
[9] P. Argyrakis and A. A. Chumak, Phys. Rev. B **66**, 054303 (2002).
[10] A. A. Chumak and C. Uebing, Ukr. J. Phys. **44**, 180 (1999).
[11] A. A. Chumak and C. Uebing, Eur. Phys. J. B **9**, 323 (1999).
[12] K. Nakazato and K. Kitahara, Prog. Theor. Phys. **64**, 2261 (1980).
[13] R. A. Tahir-Kheli and R. J. Elliott, Phys. Rev. B **27**, 844 (1983).
[14] A. A. Chumak and C. Uebing, Eur. Phys. J. B **17**, 713 (2000).
[15] P. Argyrakis, A. A. Chumak, and M. Maragakis, Phys. Rev. B **71**, 224304 (2005).
[16] A. Danani, R. Ferrando, E. Scalas, and M. Torri, Surf. Sci. **402-404**, 281 (1998).
[17] A. Danani, R. Ferrando, E. Scalas, and M. Torri, Surf. Sci. **409**, 117 (1998).
[18] P. Argyrakis, M. Maragakis, O. Chumak, and A. Zhugayevych, Phys. Rev. B **74**, 035418 (2006).
[19] C. Uebing and R. Gomer, J. Chem. Phys. **95**, 7626 (1991).